





$$xCP \frac{d\theta}{dt} = \gamma x \frac{d^2\theta}{dx^2} + \gamma y \frac{d^2\theta}{dy^2} + \gamma z \frac{d^2\theta}{dz^2} + \omega \quad (1)$$

where,

$\theta$	the variation of the soil temperature
$\chi$	the density
$Cp$	the specific heat
$T$	the time
$\lambda_x, \lambda_y, \lambda_z$	the thermal capacity in 3D
$\omega$	represents the heat produced or lost within the Rock (usually $\omega = 0$ ).

If we consider that the density, the heat capacity and the thermal conductivity are constant and identical in any point of the soil, the equation is written:

$$\frac{d\theta}{dt} = \frac{\gamma}{xCP} \frac{d^2\theta}{dx^2} \quad (2)$$

where,

$E$	the depth by taking the surface as the origin.
$\frac{\gamma}{xCP}$	the thermal diffusivity of the soil. We install $\alpha = \frac{\gamma}{xCP}$ .

We obtain a particular solution of the equation (1) if it is assumed that the temperature of the soil to infinite depth is equal to the average of the variations of the external temperature.

$$\theta(\infty, t) = 0 \quad (3)$$

This assumption is based on the fact that the temperature of the groundwater at "1 m or 2 m" of depth is very close to the annual average of the temperatures of the air outside [15]. It admits that the temperature of the air at the surface of the soil varies so sine wave, with period T and an amplitude A. at time t1, the temperature of the air will be determined by the equation:

$$\theta(0, t1) = A \cos\left(\frac{2\pi t1}{T}\right) \quad (4)$$

At the same time t1, the temperature of the soil to a depth E will be determined by an equation of the following form:

$$\theta(E, t1) = \theta m + Aa \cdot \cos(\omega t1 - \phi) \quad (5)$$

With

$\omega = \frac{2\pi}{T}$	pulse of the phenomenon of period t
$\theta m$	average soil temperature during a period of variation (assumed to be the same at all depths)
$A$	has depreciation of the Amplitude
$\phi$	dephasing phase difference (delay) of the thermal wave

We have seen that  $\theta m$  may be assimilated to the annual average of the temperatures of the air. The depreciation and dephasing are given by the following relationships:

$$a = \theta \cdot E \sqrt{\frac{\pi}{\alpha T}}$$

$$\phi = E \sqrt{\frac{\pi}{\alpha T}}$$

The variations depend on the thermal properties of the soil, of the periodicity of the phenomenon considered and depth.

$T$	period in hours
$a$	thermal diffusivity of the soil in m <sup>2</sup> /h

The dephasing  $E \sqrt{\frac{\pi}{\alpha T}}$  Is expressed in radians.

To obtain its value in time, it is necessary to multiply the result by either  $\frac{T}{2\pi}$ .

$$\phi = \frac{T}{2\pi} \cdot E \sqrt{\frac{\pi}{\alpha T}} - \frac{1}{2} E \sqrt{\frac{T}{\alpha T}} \quad (6)$$

The equation of the variation of the temperature in the soil becomes therefore:

$$\theta(E, t1) = \theta m + Aa E \sqrt{\frac{\pi}{\alpha T}} \cos\left(\frac{2\pi}{T} t1 - \frac{1}{2} E \sqrt{\frac{T}{\alpha T}}\right) \quad (7)$$

This variation has a wavelength of  $2\sqrt{\pi \alpha T}$

To a depth equivalent to this wavelength, the dephasing is a full period  $\phi = T$  and the temperature is practically stabilized to the annual average of the temperatures of the air outside. This formula allows, when it knows the parameters, to determine the temperature of the soil at different depths for each season, the multiple GPR models due to its simplicity and flexibility identify WEDM-HS process with measurement noise [16].

To simplify the calculations, we are writing the equation of the variation of the temperature in the soil form:

$$\theta_{soil} = \theta m + \sum_{j=1}^N A_T(j) \cdot [\sin(\omega(j)T - \phi_T(j))] \quad (8)$$

$$\omega = \frac{2\pi}{T}$$

and

$$\phi_T = E \sqrt{\frac{\pi}{\alpha T}}$$

$$\theta_{soil} = \theta m + \sum_{j=1}^{N=1061} A_T(j) \cdot [\sin(\frac{2\pi}{T}(j)t(j) - E \sqrt{\frac{\pi}{\alpha T}}(j))] \quad (9)$$

$$\theta_{soil} = \theta m_{day1} + \sum_{j=1}^{N=1} A_{day1} \cdot [\sin(\frac{2\pi}{T}(day1)t(day1) - E \sqrt{\frac{\pi}{\alpha T}}(day1))] \quad (10)$$

$$\theta_{soil} = \theta m_{day1061} + \sum_{j=1061}^{N=1061} A_{day1061} \cdot [\sin(\frac{2\pi}{T}(day1061)t(day1061) - E \sqrt{\frac{\pi}{\alpha T}}(day1061))] \quad (11)$$

$$\theta_{soil} = \theta m_{day1061} + \sum_{j=1061}^{N=1061} A_{day1061} \cdot [\sin(\frac{2\pi}{T}(day1061)t(day1061) - E \sqrt{\frac{\pi}{\alpha T}}(day1061))] \quad (12)$$

The equation of the Curve written as:

$$y = A \sin(P1(\frac{x-xc}{w})) \quad (13)$$

where,  $A=1$ ,  $w=1$ .

$$y = \sin(P1(x - xc)) \quad (14)$$

We have

$$\Pi=3.14$$

$$\alpha=8.3910^{-7} \text{ (diffusivity of soil)}$$

$$T=8766 \text{ h}$$

$$t_{day}=1061 \text{ day} = 25505.45 \text{ h} = 91819620 \text{ second}$$

$$\alpha T=21399078 \cdot 10^{-9}$$

The final equation of the Curve written as:

$$\theta_{soil} = \theta m \text{ day} 1 + \sum_{j=1}^{N=1} A_{day1} \cdot [\sin(\frac{2\pi}{T}(\text{day}1) t(\text{day}1)) - 0 \sqrt{\frac{\pi}{\alpha T}}(\text{day}1))] \quad (15)$$

$$\theta_{soil} = \theta m \text{ day} 1061 + \sum_{j=1061}^{N=1061} A_{day1061} \cdot [\sin(\frac{2\pi}{T}(\text{day}1061) t(\text{day}1061)) - 0 \sqrt{\frac{\pi}{\alpha T}}(\text{day}1061))] \quad (16)$$

### 3. RESULTS AND DISCUSSIONS

The soil temperature variation equation assumes that the surface temperature can be admitted to the sinusoidal annual variation, and that the earth is a homogeneous medium. In reality, these conditions are never met. Soils are not homogeneous; they are made up of elements of mineral origin and of organic origin, but also of water and air. The thermal characteristics of the soils depend on the nature of their constituents, their respective proportion and their arrangement. More a soil is "airy", the less it will lead the heat and the less it will present of inertia to the warming and cooling (case of the loess for example).

The measures of the soils thermal characteristics are difficult to achieve in situ with the solid probes, hollow, because the temperature gradients cause movements of moisture that distort the results.

The RMSE represent the difference between the predicted values estimated by the model and the measured values. In fact, RMSE identifies the model's accuracy calculated (Figure 3 and 4).

The performance of RBF models is judged by comparing the estimated values with the measured values using different statistical indexes (Figures 5 and 6) such as Root Mean Square Error "RMSE=0.0029", Relative Square Error (RRMSE), Determination Coefficient ( $r^2$ ) and Correlation Coefficient "99,05%". Mean absolute bias error "MABE=0.0021".

The heat flow distribution exhibits significant regional variations in general, are related to the local geological structure. The southern area, some relationships with extensional Miocene–Pliocene–Quaternary volcanism suggest an association with recent mantle thermal events.

Evaluation of heat, using temperature measurements (probes temperature soil) and various rock-porosity data reveal an important heat associated with the Algerian Sahara basins (Figure 7). The soil temperatures correlate well with solar energy.

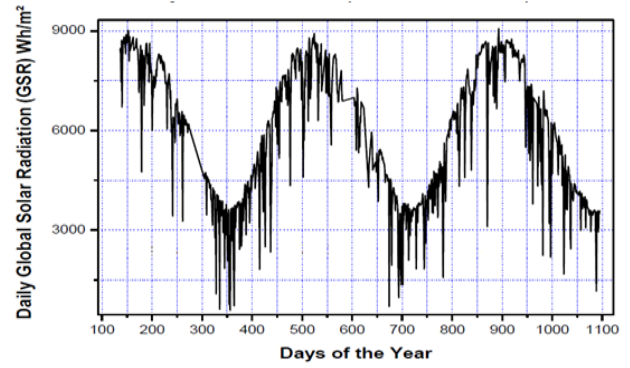


Figure 3. The global solar radiation (GSR)

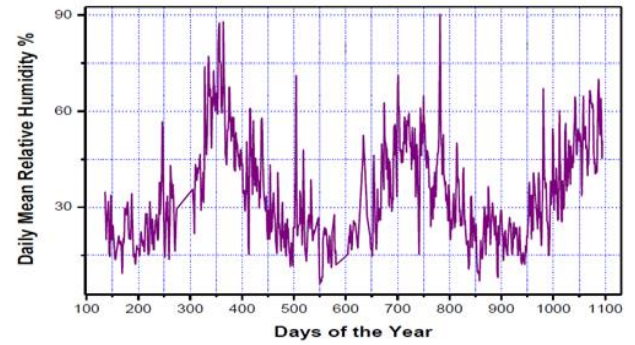


Figure 4. Variation of the humidity

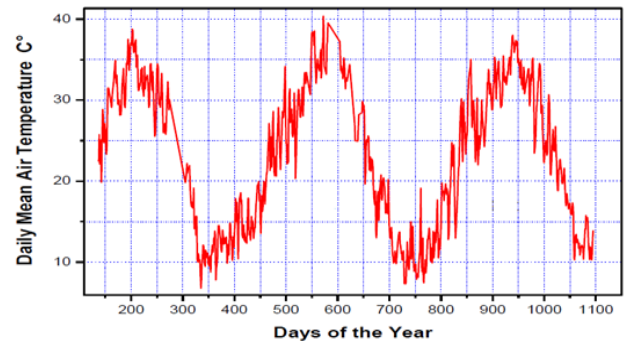


Figure 5. Measured air temperatures

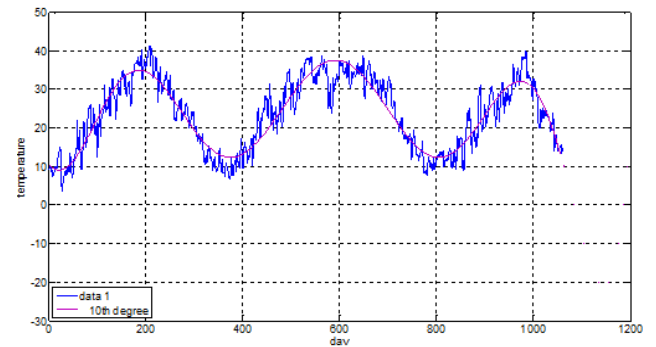


Figure 6. Predicted Soil Temperature based on meteorological data at "E=0 m"

The amplitude of the temperature signal decreases as the depth increases and beyond a distance equal to four times the depth of penetration, the soil temperature stabilizes around the average annual temperature of the surface of the earth ground.

Note also that the phase shift is inversely proportional to the thermal diffusivity of the soil (Table 1).



**Figure 7.** Soil temperature Probes (S1, S2, S3, S4, S5, S6), implanted every “0.20 m”

**Table 1.** Soil temperature, probes measurements

probes	S1-S2	S3-S4	S5	S6
temperature	18°C to 30°C	32°C to 35°C	15°C to 28°C	8°C to 25°C

The study shows that the penetration depths of the temperature signal take a period of one year greater than one meter for the limestone soil. For thermal comfort we suggest for future uses of hot air, according to the results obtained, all the depth spreads between “0 m and 0.40 m”, that the temperatures is on average of “35°C”, is the most ideal for this experimentation and for cold air we suggest the depth of “0.80 m” that the temperatures decreases is below “10°C” (Figure 8).

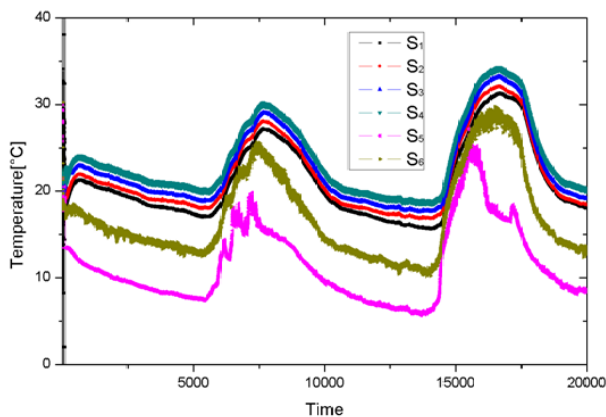


**Figure 8.** Soil Temperature measured ((S1.S2) at “E=0 m”, (S3) at “E= 0.20 m”, (S4) at “E= 0.40 m”, (S5) at “E= 0.60 m”, (S6) at “E=0.80 m”

In order to quantify the energy potential, which is immediately available for direct uses, we have made a preliminary assessment of the heat released by Canadian wells.

#### 4. CONCLUSION

The prospects for exploiting this geothermal potential are very encouraging in Ghardaia’s territory. This thermal source

makes it possible to develop agriculture under greenhouses (heating greenhouse) and even to heat the premises and homes. In this study, we used: day of the year, day length, average daily temperature, average daily relative humidity, global solar radiation measurements from the Ghardaia City radio station. On the other hand, we have estimated the temperature of the soil, for which soil probes have been inoculated at different depths. The results obtained are very satisfactory because of the strong correlation between the input (air temperature, solar radiation) and the output (soil heat). The examination carried out showed a significant effect of input parameters on the accuracy of soil temperature measurements. It has also been shown that soil temperature evaluated by solar radiation or by RBF models and those measured by probes offer close information and perfect correlations. These results allow us to use the RBF (direct, diffuse) model in areas where probes are not available or in the event of deterioration in reliability measures due to calibration problems that occur after years. The average fluctuation of the temperature at “0.40 m” meter depth is between “17.43 °C and 29.90 °C”; it represents the range of thermal comfort for the case of this study in semi-arid climate. It represents the temperature trapped in the soil all year round. We recommend using more resources from the temperatures of the basement to improve food production, especially the use of greenhouses outside the periods, in this case the climate required in these heated greenhouses to enhance growth. In the perspective of this work, we will study the applicability of this model to different soil types (bare soil and grass soil).

#### ACKNOWLEDGMENT

The author would like gratefully acknowledges the Unité de Recherche Appliquée en Energies Renouvelables (Applied Research Unit in Renewable Energies), URAER, Centre de Développement des Energies Renouvelables, CDER, 47133, Ghardaïa, Algeria, For their help and suggestions.

#### REFERENCES

- [1] Bastola, H., Peterson, E.W. (2016). Heat tracing to examine seasonal groundwater flow beneath a low-gradient stream in rural central Illinois, USA. *Hydrogeology Journal*, 24(1): 181-194. <https://doi.org/10.1007/s10040-015-1320-8>
- [2] Shamshirband, S., Mohammadi, K., Chen, H., Samy, G.N., Petković, D., Ma, C. (2015). Daily global solar radiation prediction from air temperatures using kernel extreme learning machine: A case study for Iran. *Journal of Atmospheric and Solar- Terrestrial Physics*, 134: 109-117. <https://doi.org/10.1016/j.jastp.2015.09.014>
- [3] Kusuda, T., Achenbach, P.R. (1965). Earth temperature and thermal diffusivity at selected stations in the United States (No. NBS-8972). National Bureau of Standards Gaithersburg MD.
- [4] Chen, J.L., Li, G.S., Wu, S.J. (2013). Assessing the potential of support vector machine for estimating daily solar radiation using sunshine duration. *Energy Conversion and Management*, 75: 311-318. <https://doi.org/10.1016/j.enconman.2013.06.034>
- [5] Molz, F.J., Parr, A.D., Andersen, P.F., Lucido, V.D., Warman, J.C. (1979). Thermal energy storage in a

- confined aquifer: Experimental results. *Water Resources Research*, 15: 1509-1514. <https://doi.org/10.1029/WR015i006p01509>
- [6] Voigt, H.D., Haefner, F. (1987). Heat transfer in aquifer with finite caprock thickness during a thermal injection process. *Water Resources Research*, 23: 2286-2292. <https://doi.org/10.1029/WR023i012p02286>
- [7] Guermoui, M., Mekhalfi, M.L., Ferroudji, K. (2013). Heart sounds analysis using wavelets responses and support vector machines. 2013 8th International Workshop on Systems, Signal Processing and their Applications (WoSSPA), pp. 233-238. <https://doi.org/10.1109/WoSSPA.2013.6602368>
- [8] Guendouz, A. (1985). Contribution to the geochemical and isotopic study of the deep aquifers of Sahara northeastern north (Algeria). Postgraduate Thesis Presented at the University of Paris -South, p. 243.
- [9] Fournier, R.O., Truesdell, A.H. (1973). An empirical Na, K, Cation thermometer for natural waters. *Geochimica et Cosmochimica Acta*, 37(5): 1255-1275. [https://doi.org/10.1016/0016-7037\(73\)90060-4](https://doi.org/10.1016/0016-7037(73)90060-4)
- [10] Şenkal, O., Kuleli, T. (2009). Estimation of solar radiation over Turkey using artificial neural network and satellite data. *Applied Energy*, 86(7): 1222-1228. <https://doi.org/10.1016/j.apenergy.2008.06.003>
- [11] Fabre, J. (1976). Introduction to the geology of the Algerian Sahara and neighboring regions. Soc. Nat. Ed. SNED, Algiers, p. 142.
- [12] Suykens, J.A., Vandewalle, J. (1999). Least squares support vector machine classifiers. *Neural Processing Letters*, 9(3): 293-300. <https://doi.org/10.1023/A:101862860>
- [13] Wang, J., Bras, R.L. (1999). Ground heat flux estimated from surface soil temperature. *Journal of Hydrology*, 216(3-4): 214-226. [https://doi.org/10.1016/S0022-1694\(99\)00008-6](https://doi.org/10.1016/S0022-1694(99)00008-6)
- [14] Chabert, F. (1980). Thermal environment of semi-buried structures. Excerpt from Frédéric Chabert's thesis "Habitat buried". Educational Pedagogical Unit ABC Group.
- [15] Gringarten, A.C., Landel, PA, Menjoz, A., Sauty, J.P (1979). Long-term groundwater storage of low-calorie calories for habitat. Office of Geological and Mining Research, Report No. 79 SGN 683 HYD, Orleans.
- [16] Yuan, J., Wang, K., Yu, T., Fang, M.L. (2008). Reliable multi-objective optimization of high-speed WEDM process based on Gaussian process regression. *International Journal of Machine Tools and Manufacture*, 48(1): 47-60. <https://doi.org/10.1016/j.ijmachtools.2007.07.011>